AJNR

Dynamic, Contrast-Enhanced CT of Human Brain Tumors: Quantitative Assessment of Blood Volume, Blood Flow, and Microvascular Permeability: Report of Two Cases

Heidi C. Roberts, Timothy P.L. Roberts, Ting-Yim Lee and William P. Dillon

AJNR Am J Neuroradiol 2002, 23 (5) 828-832
http://www.ajnr.org/content/23/5/828

AJNR Am J Neuroradiol 23:828–832, May 2002

Case Report

Dynamic, Contrast-Enhanced CT of Human Brain Tumors: Quantitative Assessment of Blood Volume, Blood Flow, and Microvascular Permeability: Report of Two Cases

Heidi C. Roberts, Timothy P.L. Roberts, Ting-Yim Lee, and William P. Dillon

Summary: We present two patients with metastatic brain tumors who underwent dynamic contrast-enhanced CT that yielded estimates of blood volume, blood flow, and microvascular permeability. For one patient, these CT-based quantifications were compared with contrast-enhanced MR-based assessments of fractional blood volume and permeability. Regional blood volume heterogeneity patterns were consistent between both CT- and MR imaging-based mapping. Permeability variations across the tumor, however, were less consistent, perhaps because of differences between ionic and non-ionic contrast agents. The advantages of dynamic contrast-enhanced CT in comparison with dynamic, contrast-enhanced MR imaging for microvascular quantifications are its availability and lower costs, applicability in the presence of MR imaging contraindications, and potentially more accurate analyses. The disadvantages are its limited anatomic coverage, radiation exposure, and the need for injection of a contrast agent.

Malignant tumors, whether primary tumors or metastases, are commonly characterized by neovascularity and increased angiogenic activity (1, 2). As a result, tumors may have a higher proportion of immature, and consequently hyperpermeable, vessels (3–5). Both for the assessment of tumor malignancy at initial presentation and for tumor monitoring during treatment and follow-up, there is a need for noninvasive methods to assess tumor biology in vivo. Especially with the ongoing development of anti-angiogenic therapeutic pharmaceuticals, a noninvasive, quantitative, and physiologically sensitive tool to characterize tissue microvasculature is desired. Dynamic, contrast-enhanced MR imaging has been implemented for the quantification of cerebral blood volume (CBV) and microvascular permeability (PS) (permeability surface area product) both in animal models (6–9) and, more recently, in human brain tumors (10, 11). In human gliomas, estimates of PS have been shown to be predictive of the pathologic grade (10, 11) and to correlate with the mitotic activity of a tumor (11). The application of MR imaging is often limited, however, by its availability, expense, and the appearance of postsurgical artifacts. Recently, dynamic contrast-enhanced CT has been implemented in animal models of brain tumors to quantify and compute maps of CBV, cerebral blood flow (CBF), and PS (12). We present the results of this technique in two malignant human brain tumors and in one case compare the results with those of dynamic contrast-enhanced MR imaging microvascular mapping.

Received August 6, 2001; accepted after revision December 6.

From the Department of Radiology (H.C.R., T.P.L.R., W.P.D.), University of California, San Francisco, San Francisco, CA, and the Robarts Research Institute (T.-Y.L.), London, Ontario, Canada.

Address reprint requests to Heidi C. Roberts, MD, Department of Medical Imaging, Toronto General Hospital/UHN, Toronto, Ontario, Canada MSG 2C4.

Methods

Patients

Patient 1 was a 71-year-old patient who had undergone gamma knife therapy for three melanoma metastatic foci to the brain and who presented with a seizure. CT of the brain revealed a focus compatible with a metastasis located in the left posterior superior parietal lobe (Fig 1). High attenuation on an unenhanced CT scan indicated hemorrhage in the tumor.

Patient 2 was a 50-year-old woman with a history of adenocarcinoma of the proximal rectum and both pulmonary and hepatic metastases. She presented with a 10-day history of increasing left arm and left leg weakness. CT of the brain revealed multiple, bilateral metastatic lesions; one of the lesions measured 4.5 cm in diameter (Fig 2). Subsequently, MR imaging was performed. The MR imaging sequence for microvascular quantifications was performed and kinetically analyzed as previously published (10).

CT Protocol

For each patient, a representative lesion underwent a dynamic contrast-enhanced scanning series on a multidetector CT scanner (Lightspeed; GE Medical Systems, Milwaukee, WI) using the following parameters: 80 kV, 190 mA, 512 × 512 matrix, and a standard algorithm. Scans were acquired after a bolus injection of 100 cc (4 cc/s) of non-ionic contrast agent (Omnipaque300, Nycomed), every 2 s for the first 80 s and then every 20 s, for a total data acquisition duration of 5.5 min. Two 1-cm-thick sections were reconstructed. Regions of interest were drawn, and density changes in blood and tissue were kinetically analyzed using CT Perfusion 2 software (GEMS), which yields parameter maps of fractional tissue blood volume (CBV [mL/1000 g], CBF [mL/100 g/min]) and PS (mL/100 g/min), based on deconvolution between arterial and regional tissue enhancement curves with a distributed parameter model (13, 14). CBV and CBF mapping has proven efficacious in cases of acute cerebral ischemia (15, 16), in animal models, in patients with benign and malignant disturbance of cerebral perfusion (17), and in benign brain tumors without blood-brain barrier disruption (18). CT Perfusion 2 software extends the application of dynamic CT to

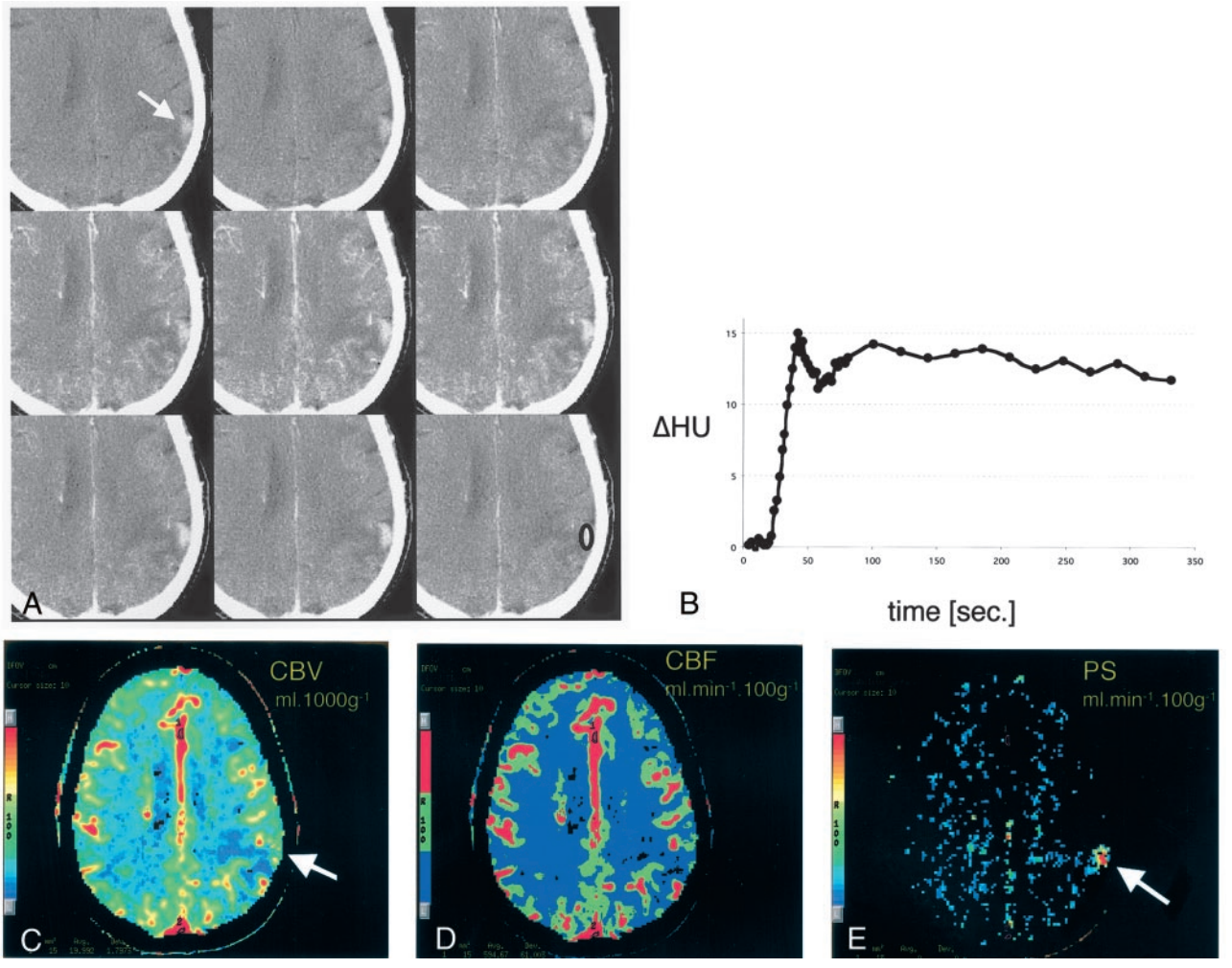

FIG. 1. CT scans and data analysis obtained from patient 1.

A, Representative images from the dynamic contrast-enhanced CT study. *Top row*, Before the administration of contrast material, a subtle tumoral hyperattenuation indicates hemorrhage (*arrow*). *Middle row*, After the injection of contrast agent , the tumor is immediately and strongly enhancing. *Bottom row*, The tumor remains hyperattenuating even after the contrast agent washes out.

B, Time-attenuation curve of the tumor from the ROI in the *bottom right image* in *A*. Strong enhancement of approximately 15 HU is present during the first pass. A slight decrease in tumoral attenuation is followed by steady enhancement during the equilibrium phase. Contrast-agent washout is not observed during the studied period of approximately 5 minutes.

C–E, Pixel-by-pixel parameter maps of CBV (*C*), CBF (*D*) and PS area (*E*) in the section in *A*. CBV is slightly increased in the tumor and decreased in the surrounding edematous tissue. No increase in blood flow is seen. Tumoral conspicuity is highest on the PS map (*arrow*), against the near-zero permeability of the normal brain tissue.

include estimates of PS as a putative, quantitative indicator of blood-brain barrier disruption.

Results

For patient 1, the tumor showed intense enhancement on both early and late contrast-enhanced scans (Fig 1A). Region of interest measurements in the tumor revealed an initial contrast peak (Fig 1B). The high PS of the tumor resulted in a transendothelial diffusion of the contrast agent into the tissue interstitium, which can be recognized by the very slight decline of the signal intensity after the first pass (compared with the substantial decline to near baseline seen with an intact blood-brain barrier), and a consequent increase of tissue density during the equilibrium phase (Fig 1B). The pixel-by-pixel analysis of the contrast agent kinetics reveal that compared with normal gray matter, the tumor CBV is subtly increased (from 5% to 8%) (Fig 1C and D) and CBF normal (Fig 1C and E), whereas the surrounding edematous tissue shows decreased CBV and CBF. PS (Fig 1C, *bottom*, *arrow*) was characteristically elevated in the tumor (>10 mL/100 g/min) compared with normal brain tissue, which had approximately zero permeability (Fig 1E).

For patient 2, as evident from the CT scans (Fig 2A) and the region of interest display (Fig 2B), the tumor showed a contrast agent enhancement pattern similar to that of the tumor in patient 1: an early peak and then an almost complete lack of density decrease after the first pass, attributable to microvascular hyperpermeability. The perfusion/permeability parameter maps depict the tissue heterogeneity within the large tumor, with both CBV and CBF being higher in

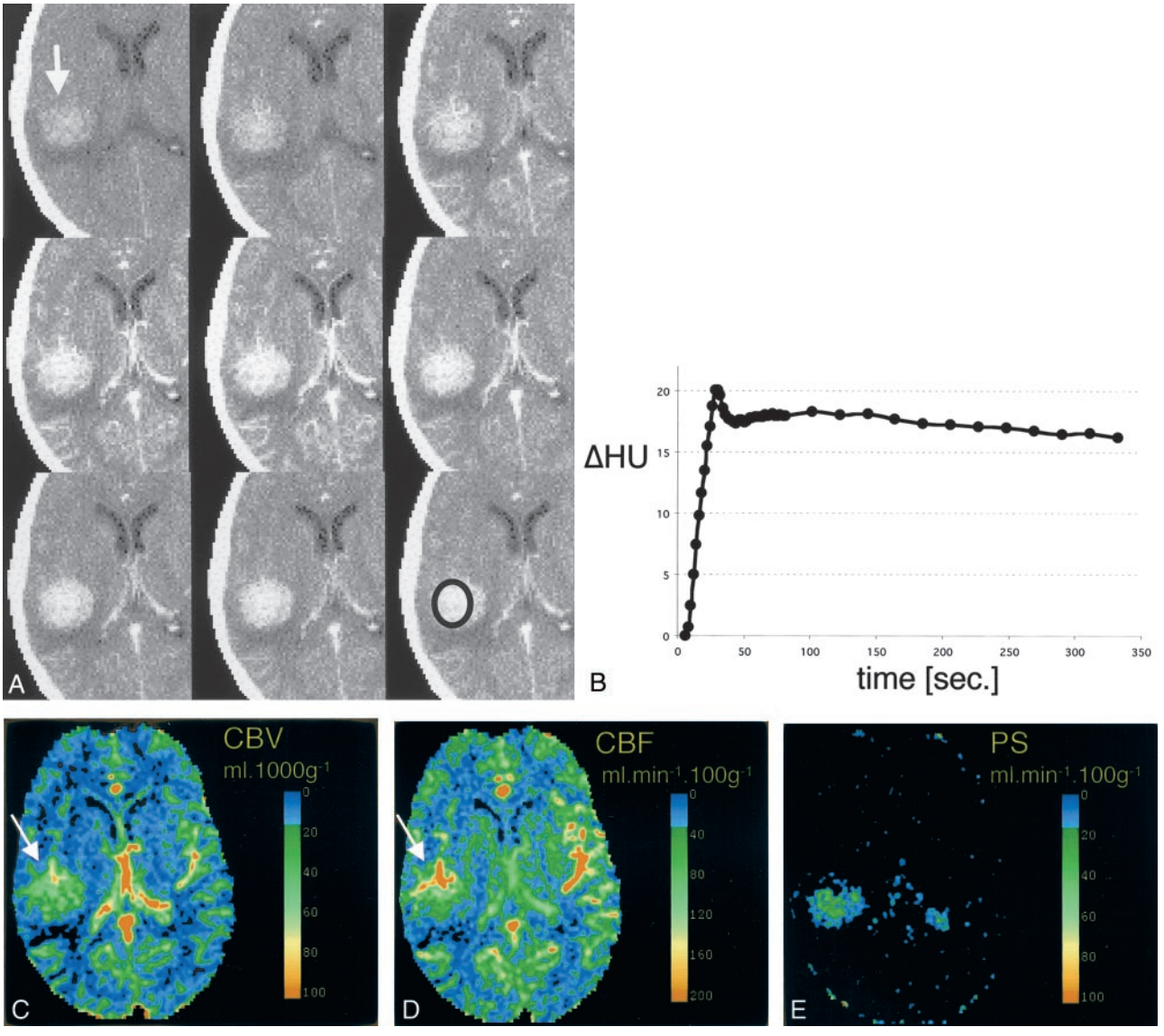

FIG. 2. CT scans and data analysis obtained from patient 2.

A, Representative images from the dynamic contrast-enhanced CT study. *Top row*, Before contrast administration, hyperattenuation within the tumor indicates hemorrhage (*arrow*). *Middle row*, After the injection of contrast agent, the tumor is immediately and strongly enhancing. *Bottom row*, The tumor remains hyperattenuated even after the contrast agent has washed out.

B, Time-density curve of the tumor, from the ROI in the *bottom right image* in *A*. Strong enhancement of approximately 20 HU is present during first pass. A slight decrease in tumoral attenuation is followed by a steady enhancement during the equilibrium phase. Contrast-agent washout is not observed during the studied period.

C–E, Pixel-by-pixel parameter maps of CBV (*C*), CBF (*D*) and PS area (*E*) from the section in *A*. Both CBV and CBF are markedly increased in the tumor; this is most pronounced in the more anterior tumoral areas (*arrows*). In vascularized tumor tissue, CBF is as high as in the CBF in the contralateral insular vessels. Tumor conspicuity is highest on the PS map, with near-zero permeability of the normal brain tissue. (The contralateral area of high PS indicates the plexus, which does not have a blood-brain barrier and is inherently permeable to the contrast agent).

the more anterior parts of the tumor (Fig 2C and D). In highly vascularized areas, CBF reaches values comparable with those of vascular structures. As in patient 1, tumor conspicuity is most obvious on the permeability maps (>40 mL/100 g/min) compared with the approximately zero permeability of the surrounding tissue (Fig 2E).

The dynamic contrast-enhanced MR imaging study confirms the strong enhancement of the tumor (Fig 3A). The blood volume map (Fig 3B) shows the same distribution of elevated blood volume within the tumor as was shown by the CT study: blood volume is higher in the more anterior parts of the tumor. Permeability, however, was highest in the tumor center on the CT study (Fig 2E) but highest in the tumor periphery on the MR imaging study (Fig 3C).

Discussion

CT permeability studies combine the continuous dynamic data acquisition of a single section with IV administration of an iodinated contrast agent bolus

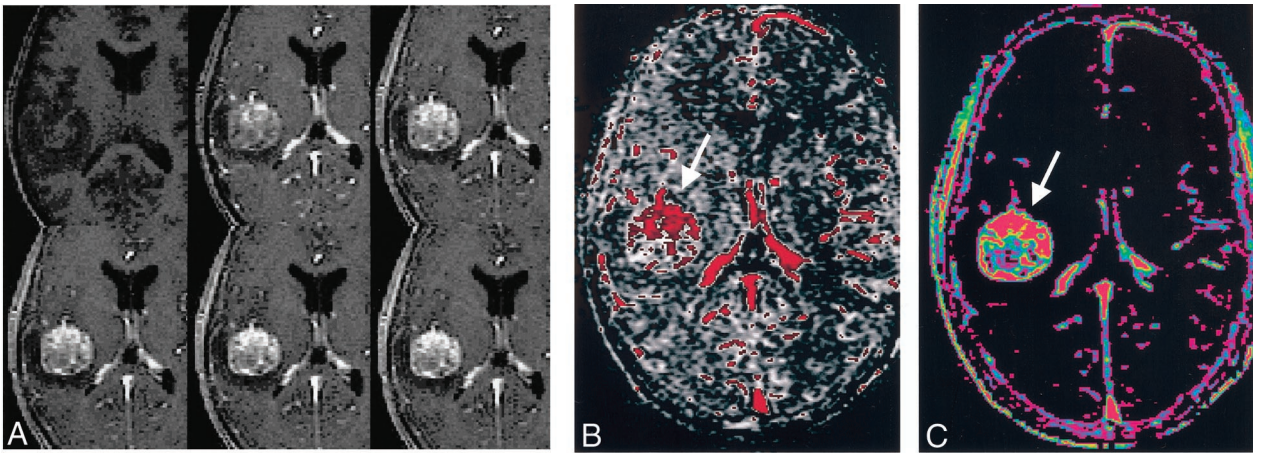

FIG. 3. *A*, Representative images from the dynamic contrast-enhanced MR study in the patient in Figure 2. As seen on the CT scans (Fig 2), contrast enhancement is strong and immediate, and wash-out is slow. After the injection of contrast agent , the tumor is immediately and strongly enhancing (*top row*, *middle* and *right images*), and it remains hyperintense relative to the vascular signal intensity (*bottom row*).

B and *C*, Pixel-by-pixel parameter maps of CBV (*B*) and PS (*C*) from the section in *A*. As seen on the CT maps, blood volume is increased mostly in the more anterior tumor areas (*B, arrow*). Permeability is highest in the more anterior and peripheral tumor areas (*C, arrow*) as well.

and appropriate kinetic modeling of the contrast agent transit through the tissue. This technique allows noninvasive determination of the tumor blood volume, the blood flow, and a measure of the permeability of tumor vessels. We present the use of a dynamic, contrast-enhanced CT method in two human brain tumors for the quantification of CBF, CBV, and PS. This is based on a bolus contrast agent injection and image acquisition beyond the first pass circulation of contrast agent. One of those cases is compared with a similar, MR imaging-based technique.

The noninvasive investigation of the tissue microvasculature has previously been the focus of attention. It is generally acknowledged that such a method can be used to estimate the angiogenic activity of a tumor, and thus its biologic aggressiveness, and to follow tumor response to treatment. In particular, it may serve as a surrogate outcome measure for antiangiogenic treatment. Moreover, permeability measurements can direct the biopsy of the most malignant representative in a tumor for histologic evaluation (10). For the two patients whose cases are presented herein, permeability maps were more conspicuous for showing malignant tumors compared with CBV and CBF, which were slightly increased relative to the surrounding tissue. The presence of *hyper*permeability seemed to be a specific effect: a positive PS was evident only in the malignant tumor, not in the surrounding tissue with intact blood-brain barrier.

Although MR imaging studies of permeability are relatively accessible and do not require sophisticated hardware, there are some inherent disadvantages associated with the kinetic analysis of the acquired data. Mainly, the correlation between the signal intensity and the contrast agent concentration is not linear, impairing a correct analysis of the microvascular characteristics. The most appropriate measure to correct for this effect (ie, calculating the changes in relaxation rate $\Delta[1/T_1]$ as an indicator of tracer concentration, rather than relying on signal intensity changes, Δ[SI]), is associated with an increase in scan time and is thus not practical. Furthermore, even $\Delta(1/T_1)$ is nonetheless an approximation, typically assuming homogeneity of tissue type, or at least "fast water exchange," within each image voxel. Such fast exchange assumptions are contentious, especially in the brain (19).

Considering the linear relationship between the density changes and contrast agent concentration and the lack of confounding sensitivity to flow, CT-based quantifications potentially offer a more accurate representation of the tissue microvasculature compared with MR imaging. The CT-based methodology used for the two patients whose cases are presented herein has previously been validated in animal models (12). The authors found this technique to be both accurate and precise in its quantitation of flow parameters, using a microsphere technique as the reference standard. Combined with a higher spatial resolution than that of MR imaging and no susceptibility artifacts, CT may be more suitable for the noninvasive assessment of tumor malignancy and as a surrogate outcome marker for monitoring treatment effects, particularly anti-angiogenesis treatment. Other possible applications for microvascular assessment using dynamic contrast-enhanced CT may be differentiation of the most malignant region of tumor before conducting stereotactic biopsy and differentiation of radiation necrosis and postsurgical scar tissue from recurring tumor.

Radiation exposure and iodinated contrast agents present considerable tradeoffs when comparing CT with MR imaging-based permeability techniques. The effective dose equivalent (20) of a dynamic CT study, as reported herein, has been estimated to be 4.03 mSv, and the skin dose has been reported to be 64.6 rad (unpublished data). This effective dose equivalent is approximately twice as high as the radiation dose from routine CT of the brain (1.5 mSv) (21). The risk

of reaction to the contrast agent is low when using nonionic agents but is higher than the risk associated with MR imaging contrast agents. A considerable disadvantage of CT permeability measurements compared with MR imaging-based approaches is the limited anatomic coverage of CT. Even the use of multidetector scanners currently restricts the scanned volume to a maximum of 2 cm; however, the temporal resolution of MR imaging permeability studies (approximately 30 s) (10) is far exceeded by that of CT. An improved imaging approach might be to repeatedly scan a larger tumor area, several tumors, or even the whole brain by using a helical scanning mode. More studies are warranted to determine whether the potentially more accurate CT-based approach outweighs these drawbacks.

Comparing CT and MR imaging permeability maps, some inherent differences may be recognized. Whereas fractional blood volume is a parameter inherent to the tissue and should not change with the probe used to measure CBV (and seems to be comparable on the CT and MR imaging CBV maps) (Fig 2C and E), PS is always specific to a particular tracer. For noninvasive imaging, this means that the permeability of the microvasculature to the CT contrast agent is not necessarily identical to the permeability of an MR imaging contrast agent. The permeability depends on several factors but mainly the size, shape, and charge of the contrast agent. The CT and MR imaging contrast agents used do not differ considerably in their molecular weight; however, the different charge of the nonionic CT contrast agent compared with the ionic MR imaging contrast agent (Omniscan, Nycomed) may be responsible for some of the differences in PS in the tumor of patient 2. Moreover, the temporal resolution, section thickness, and angulation of the acquisition differed somewhat between the CT and MR imaging studies of patient 2. This suggests that follow-up studies to monitor treatment should be conducted using the same technique throughout, with considerable attention to study-to-study image registration, and that CT and MR imaging are not necessarily interchangeable modalities.

In summary, CT-based microvascular quantifications present an appealing alternative to MR imaging-based techniques. They are applicable in the presence of susceptibility artifacts or general contraindications for MR imaging and potentially offer more accurate results. However, mainly because of the limited anatomic coverage and the inherent risk of radiation exposure and injection of contrast agent, CT is unlikely to generally replace MR imaging for the noninvasive assessment of human brain tumor biology.

References

1. Jain RK. **Vascular and interstitial barriers to delivery of therapeutic agents in tumors.** *Cancer Metastasis Rev* 1990;9:253–266
2. Folkman J. **The role of angiogenesis in tumor growth.** *Semin Cancer Biol* 1992;3:65–71
3. Hirata A, Baluk P, Fujiwara T, McDonald DM. **Location of focal silver staining at endothelial gaps in inflamed venules examined by scanning electron microscopy.** *Am J Physiol* 1995;269:L403–L418
4. Nugent LJ, Jain RK. **Extravascular diffusion in normal and neoplastic tissues.** *Cancer Res* 1984;44:238–244
5. Jain RK, Gerlowski LE. **Extravascular transport in normal and tumor tissues.** *Crit Rev Oncol Hematol* 1986;5:115–170
6. van Dijke CF, Brasch RC, Roberts TP, et al. **Mammary carcinoma model: correlation of macromolecular contrast-enhanced MR imaging characterizations of tumor microvasculature and histologic capillary density.** *Radiology* 1996;198:813–818
7. Schwickert HC, Stiskal M, Roberts et al. **Contrast-enhanced MR imaging assessment of tumor capillary permeability: effect of irradiation on delivery of chemotherapy.** *Radiology* 1996;198:893–898
8. Daldrup H, Shames DM, Wendland M, et al. **Correlation of dynamic contrast-enhanced MR imaging with histologic tumor grade: comparison of macromolecular and small-molecular contrast media.** *AJR Am J Roentgenol* 1998;171:941–949
9. Pham CD, Roberts TP, van Bruggen N, et al. **Magnetic resonance imaging detects suppression of tumor vascular permeability after administration of antibody to vascular endothelial growth factor.** *Cancer Invest* 1998;16:225–230
10. Roberts HC, Roberts TP, Brasch RC, Dillon WP. **Quantitative estimation of microvascular permeability in human brain tumors using dynamic contrast-enhanced MR imaging: correlation with histological grade.** *AJNR Am J Neuroradiol* 2000;21:891–899
11. Roberts HC, Roberts TP, Bollen AW, Ley S, Brasch RC, Dillon WP. **Correlation of microvascular permeability derived from dynamic contrast-enhanced MR imaging with histologic grade and tumor labeling index: a study in human brain tumors.** *Acad Radiol* 2001;8:384–391
12. Cenic A, Nabavi DG, Craen RA, Gelb AW, Lee TY. **A CT method to measure hemodynamics in brain tumors: validation and application of cerebral blood flow maps.** *AJNR Am J Neuroradiol* 2000; 21:462–470
13. Lawrence KS, Lee TY. **An adiabatic approximation to the tissue homogeneity model for water exchange in the brain: I. theoretical derivation.** *J Cereb Blood Flow Metab* 1998;18:1365–1377
14. Miles K, Charnsangavej C, Lee FT, Fishman E, Horton K, Lee TY. **Application of CT in the investigation of angiogenesis in oncology.** *Acad Radiol* 2000;7:840–850
15. Nabavi DG, Cenic A, Henderson S, Gelb AW, Lee TY. **Perfusion mapping using computed tomography allows accurate prediction of cerebral infarction in experimental brain ischemia.** *Stroke* 2001;32: 175–183
16. Lee T, Roberts H, Smith W, Johnston S, Dillon W. **Evaluation of acute stroke using multi-location dynamic CT perfusion: comparison with conventional CT.** *AJNR Am J Neuroradiol* 2001; submitted
17. Nabavi DG, Cenic A, Craen RA, et al. **CT assessment of cerebral perfusion: experimental validation and initial clinical experience.** *Radiology* 1999;213:141–149
18. Bondestam S, Halavaara JT, Jääskeläinen JE, Kinnunen JJ, Hamberg LM. **Perfusion CT of the brain in the assessment of flow alterations during brachytherapy of meningioma.** *Acta Radiol* 1999; 40:469–473
19. Donahue KM, Weisskoff RM, Burstein D. **Water diffusion and exchange as they influence contrast enhancement.** *J Magn Reson Imaging* 1997;7:102–110
20. ICRP. *Recommendations of the International Commission on Radiological Protection:* ICRP Publication 26. Oxford: Pergamon Press
21. Huda W, Sandison GA, Lee T-Y. **Patient doses from computed tomography in Manitoba from 1977 to 1987.** *Br J Radiol* 1989;62: 138–144